

Origin of the anatase to rutile conversion of metal-doped TiO₂

Sa Li and P. Jena

Department of Physics, Virginia Commonwealth University, Richmond, Virginia 23284-2000, USA

(Received 27 January 2009; revised manuscript received 26 April 2009; published 13 May 2009)

Extensive calculations using density functional theory enable us to explain the origin of the surprising room-temperature conversion of anatase to rutile phase of TiO₂ when doped with Co and Ni, but not with Cu. Contrary to earlier suggestion, neither high spin nor strain of the transition metals is found to be responsible for this phase conversion. The driving mechanism, instead, is attributed to the increased interaction between Co and Ni atoms forming a linear chain in the rutile phase. We predict that Cr and Mn which have even larger spins than Co and Ni cannot induce this phase conversion.

DOI: [10.1103/PhysRevB.79.201204](https://doi.org/10.1103/PhysRevB.79.201204)

PACS number(s): 71.10.Hf, 61.72.-y, 71.15.Nc, 75.50.Pp

Growing interest in the study of TiO₂ semiconductor stems from its current use in photovoltaics,¹ electrochromics,² sensors,³ and photocatalysis.⁴ In the ground state TiO₂ exists in the anatase phase and undergoes transition to the rutile phase at temperatures well in excess of 600 °C.⁵ Since the optical and electrical properties of anatase and rutile TiO₂ are distinctly different, it is desirable to be able to control phase content and conversion between these two phases. In particular, it has been suggested that, due to the novel semiconducting properties of the anatase/rutile interface region, partial conversion from anatase to rutile phase may render TiO₂ with exciting photocatalytic properties.⁶⁻⁸ Consequently, there has been considerable interest⁹⁻¹¹ in finding ways to induce this phase transition at lower temperatures. In a recent paper, Gole *et al.*¹² reported the surprising room-temperature phase conversion of anatase to rutile TiO₂ by using transition-metal ions with highly unpaired electron spins. They showed that Co, and to a lesser extent Ni, accomplishes this conversion, while it does not occur when Cu is used as a dopant. The authors attributed the origin of this phase conversion to the magnetic nature of Co and Ni.

In this Rapid Communication we show that Ni in TiO₂ is nonmagnetic and Co doping continues to enable the phase conversion even after switching off the magnetic interaction. Furthermore, Cr and Mn whose atomic spins are larger than that of Co are also incapable of causing this phase transition. The origin of the phase conversion resulting from Co and Ni doping is found to be due to the increased interaction between these atoms as they form a linear chain in the rutile structure. Our studies also reveal some unusual magnetic behavior of Cu, Fe, and Cr when doped in TiO₂: nonmagnetic Cu couples ferromagnetically, ferromagnetic (FM) Fe couples antiferromagnetically, and antiferromagnetic (AFM) Cr couples ferromagnetically.

The relaxations in the lattice caused by the dopant atom(s), the total energy, and the electronic structure were calculated using Vienna *ab initio* simulation package (VASP) (Ref. 13) and the projector augmented wave (PAW) (Ref. 14) method. The PAW generalized gradient approximation (GGA) (Ref. 15) potentials with the valence states 3*d* and 4*s* for Ti, Cr, Mn, Fe, Co, Ni, and Cu and 2*s* and 2*p* for O were used. High precision calculations with a cutoff energy of 400 eV for the plane-wave basis were performed. In addition, GGA+*U* calculations with parameter values of

$U=3.0$ eV and $J=0.87$ eV (Ref. 16) for Cr, Mn, Fe, Co, Ni, and Cu 3*d* electrons were carried out. The geometries of the above supercells (ionic coordinates and *c/a* ratio) were optimized without any symmetry constraint. For sampling the irreducible wedge of the Brillouin zone we used *k*-point grids of $6 \times 6 \times 4$ and $4 \times 4 \times 8$ for the anatase and rutile tetragonal supercells, respectively. In all calculations, self-consistency was achieved with a tolerance in the total energy of at least 0.1 meV. To study the magnetic properties of metal-doped TiO₂, we carried out spin-polarized calculations including both ferromagnetic and antiferromagnetic configurations.

The anatase TiO₂ has a tetragonal structure and belongs to the space group *I41/amd* (141). In the anatase structure, each Ti atom is octahedrally bonded to six O atoms with four O atoms lying at a distance of 1.94 Å from Ti while the other two are at 1.99 Å. TiO₂ rutile structure belongs to the space group *P42/mnm* (136). In the rutile structure, each Ti is also octahedrally coordinated with O atoms with four of them lying on the (110) plane at a distance of 1.95 Å while the other two lie along the [110] direction at a distance of 1.98 Å. Our calculations show that the anatase phase is 0.998 eV lower in energy than the rutile phase at 0 K.

We first discuss dopant concentration of 6.25% where one Ti atom in the 48-atom supercell is replaced by Cr, Mn, Fe, Co, Ni, or Cu. At this concentration we found the anatase phase to be more stable than the rutile phase by 1.309, 0.795, 0.672, 0.623, 0.742, and 0.574 eV for Cr, Mn, Fe, Co, Ni, and Cu dopants, respectively. The magnetic moments at the Cr, Mn, Fe, Co, Ni, and Cu sites in the anatase phase are 1.87, 2.65, 1.73, 0.73, 0, and 0.39 μ_B and in the rutile phase are 0.61, 2.62, 1.67, 0.67, 0, and 0.63 μ_B respectively. GGA+*U* calculations lead to slightly higher magnetic moment on each dopant atom. For example, the moment of Co in anatase TiO₂ increases from 0.73 to 0.83 μ_B by means of GGA+*U* method. The magnetic behavior of Co, Mn, Fe, and Ni-doped anatase TiO₂ is similar to the findings of Park *et al.*¹⁶ The difference between numerical values of the magnetic moments calculated by us and these authors¹⁶ may be due to the use of different muffin-tin radii.

The relative phase stability changes when the dopant concentration is increased to 12.5%. Note that for this concentration, we have chosen two different sites for the dopants in both anatase and rutile structures (Fig. 1). We find that in the anatase phase, Cr, Fe, Co, Ni, and Cu atoms prefer to occupy

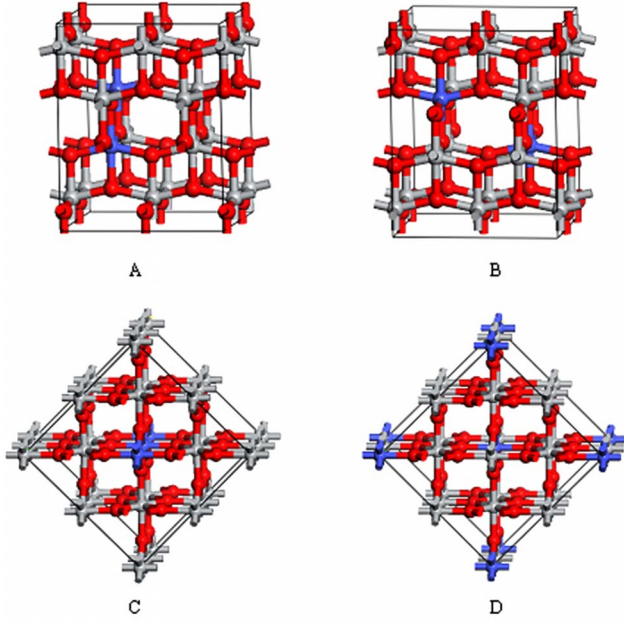


FIG. 1. (Color online) The crystal structures showing the dopant sites for 12.5% concentration in anatase TiO₂ (configurations A and B) and rutile TiO₂ (configurations C and D).

nearest-neighbor sites (configuration A) while Mn atoms prefer to remain farther away (configuration B). The $M-M$ distances are shown in Table I. When two Mn atoms are apart at the distance of 4.85 Å, AFM configuration is only 7 meV more favorable than FM configuration. In the rutile phase, however, all dopant atoms prefer to occupy nearest-neighbor sites (configuration C). In Table I we give the energy difference between the anatase and rutile phases of Ti_{1-x}M_xO₂ ($M=Cr, Mn, Fe, Co, Ni, \text{ and } Cu; x=0.125$) systems. We define this energy difference as, $\Delta E=E(\text{anatase})-E(\text{rutile})$. Here E is the total energy of a given phase and negative value for ΔE means that the anatase phase is more stable than the rutile phase. We see from Table I that Co and, to a lesser extent, Ni-doped TiO₂ favor the rutile phase as the ground state while Cr, Mn, and Cu doping have no effect on the phase conversion. GGA+ U calculations show similar

trend, even though Ni-doped system slightly favors the anatase structure. In Fe-doped TiO₂, Fe atoms couple antiferromagnetically, which is in agreement with recent findings that substitution of Fe in anatase TiO₂ does not introduce ferromagnetic ordering.¹⁷ The anatase phase is preferred for Fe doping, but the energy difference is small.

We now concentrate on the origin of the phase conversion in Co and Ni and lack of it in Cu. We note that the magnetic moment of Co, Ni, and Cu free atoms are 3, 2, and 1 μ_B , respectively. In the bulk phase Co and Ni are ferromagnetic while Cu is paramagnetic (PM). However, when doped in TiO₂, Co and Cu carry magnetic moment while Ni does not. These features can be seen from the density of states (DOS) in both the anatase and rutile phases. As an example, we present the DOS for 12.5% metal-doped rutile phase in Fig. 2. In pristine rutile TiO₂, the lower valence band (LVB) is dominated by O-2s states. The upper valence band (UVB) is composed of O-2p states and Ti-3d states. The UVB has a calculated bandwidth of 5.5 eV and is separated from the conduction band (CB) by a band gap of 1.7 eV. We see that Co-doped TiO₂ is a semimetal. It has a pseudo gap at the Fermi level in the spin down states. Addition of Ni to TiO₂ not only introduces new states at the middle of the band gap but also at the UVB. The delocalized Ni- d states hybridize strongly with O- p and Ti- d states in the UVB, thus making Ni-doped TiO₂ paramagnetic.¹⁸ Cu-doped TiO₂ behaves half-metallic, and the localized energy levels from the dopant distribute just at the UVB. In the GGA+ U calculations, Co-doped rutile TiO₂ is still a semimetal, with spin-up 3d valence bands slight moving to higher energy. We see that the mid-gap bands in Ni-doped system are broadened in the GGA+ U calculation. In contrast to the GGA results in Cu-doped TiO₂, the Fermi level falls into the gap of the Cu 3d spin-up states when GGA+ U method is used.

It has been suggested that the phase conversion in Co and Ni-doped TiO₂ could have a magnetic origin. As mentioned earlier, this cannot be the case at least for Ni since its magnetic moment is zero. Equally important, Cu-doped TiO₂ film at a concentration of approximately 10 at. % has been reported experimentally¹⁹ to be ferromagnetic at room temperature, yet it does not exhibit phase conversion. Our results show that Cu at 6.25% concentration carries a magnetic mo-

TABLE I. The GGA optimized average $M-O$ distance (Å), $M-M$ distance (Å), the magnetic moments (μ_B) at each dopant site, the preferred magnetic coupling, the energy difference (eV) between the anatase (ana) and rutile (rut) phases ($\Delta E=E_{\text{anatase}}-E_{\text{rutile}}$), and the energy difference (eV) between two dopant configurations ($\delta E=E_D-E_C$) for the dopant concentration of 12.5% shown in Fig. 1. The GGA+ U calculated energy differences are shown to compare with GGA calculations.

Dopant	$M-O$		$M-M$		μ		Coupl.		ΔE		δE (E_D-E_C)
	(Ana.)	(Rut.)	(Ana.)	(Rut.)	(Ana.)	(Rut.)	(Ana.)	(Rut.)	(GGA) ($E_{\text{ana}}-E_{\text{rut}}$)	(GGA+ U) ($E_{\text{ana}}-E_{\text{rut}}$)	
Ti	1.96	1.96	3.04	2.95	0	0	PM	PM	-0.998	-0.998	
Cr	1.91	1.92	2.90	2.95	1.95	2.02	FM	FM	-0.680	-0.636	0.223
Mn	1.89	1.91	4.85	2.95	2.64	2.63	AFM	AFM	-0.472	-0.495	0.138
Fe	1.89	1.90	2.83	2.94	1.93	1.85	AFM	AFM	-0.018	-0.057	0.578
Co	1.88	1.89	2.81	2.94	0.66	0.65	FM	FM	0.077	0.052	0.768
Ni	1.88	1.89	2.88	2.95	0	0	PM	PM	0.011	-0.046	0.453
Cu	1.93	1.95	3.03	2.96	0	0.60	PM	FM	-0.154	-0.116	0.179

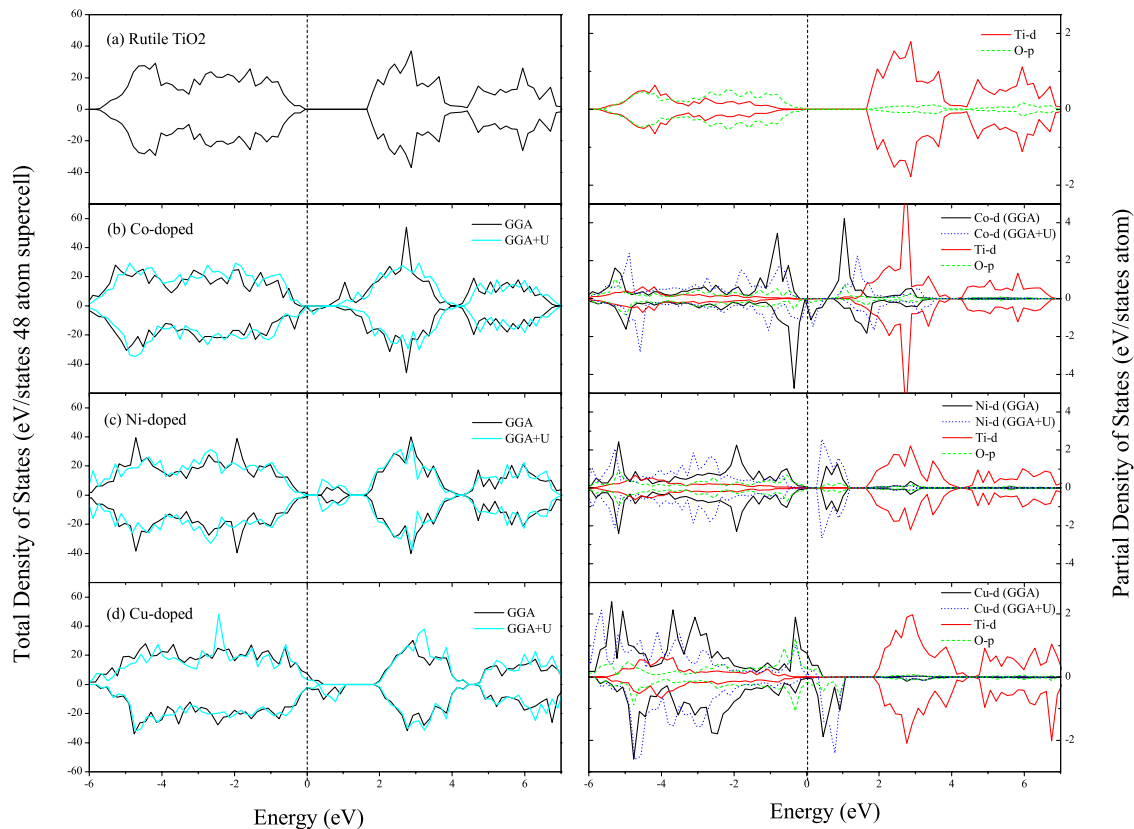


FIG. 2. (Color online) The total DOS for pristine and metal-doped rutile TiO_2 (configuration C): (a) undoped, (b) Co-doped, (c) Ni-doped, and (d) Cu-doped rutile TiO_2 structures.

ment of 0.39 and $0.63 \mu_B$ in the anatase and rutile phases, respectively. When Cu concentration increases to 12.5% , the moment on Cu in the anatase phase quenches to $0 \mu_B$ but remains at $0.60 \mu_B$ in the rutile phase. The coupling is ferromagnetic. We conclude that the magnetic signals seen experimentally in the Cu-doped TiO_2 can be directly assigned to Cu substitution at the Ti site²⁰ when Cu concentration is low. Oxygen vacancies can only enhance the moment on Cu. At 25% Cu concentration, rutile TiO_2 is found to be nonmagnetic which agrees with the calculations of Duhalde *et al.*¹⁹ However, contrary to the work of Li *et al.*,²¹ we found that 6.25% Cu-doped rutile TiO_2 is magnetic. To understand the source of this discrepancy we note that there are two PAW potentials for Cu, one incorporates the $3p$ orbitals, while the other does not. We repeated our calculations by including the $3p$ orbitals and found that when enough empty energy bands are included, the moment on Cu is $0.43 \mu_B$. Thus, we conclude that Cu-doped TiO_2 is magnetic at low concentration, but it is unable to cause the phase conversion. To further rule out the possibility that magnetism is responsible for the phase conversion in Co-doped TiO_2 , we repeated our calculation by switching off the spin polarization provision. A nonspin polarized calculation on Co-doped system for the 12.5% concentration showed that the rutile structure is still 0.172 eV lower in energy than the anatase structure.

The next possibility is that strain induced by dopants may be responsible for the observed phase conversion. To illustrate the role of strain, we note that the ionic radii of Co (+2) and Ni (+2) are, respectively, 0.74 and 0.72 \AA which

are larger than the ionic radius of Ti (+4), namely, 0.68 \AA . The ionic radius of Cu (+2), on the other hand, is 0.69 \AA which is much closer to the Ti value. This is reflected in the optimized average distance between Co-O, Ni-O, and Cu-O in the doped sample given in Table I. Note that the distances for the Co and Ni-doped systems are significantly smaller than those of Ti-O distances both in the anatase and rutile phases. For Cu-doped systems, however, the distances are much closer to the value in pristine TiO_2 . This may give the impression that strain may be responsible for the phase conversion. To see if this indeed is the case, we repeated the calculations for Co-doped TiO_2 by not allowing the supercell to relax. The rutile phase was again found to be 0.336 eV lower in energy than the anatase phase at the 12.5% concentration. Thus, phase conversion in Co doped cannot be induced by strain.

To resolve the mystery of the origin of phase transition, we note that in the rutile phase the doped atoms form a linear chain at the 12.5% concentration, thus enabling the dopant atoms to interact more strongly with each other than they can in the anatase phase. To see if this interaction can play a role, we compare the energy difference between configurations C and D (see Fig. 1). We find that all the three dopants—namely, Co, Ni, and Cu—prefer to form a linear chain structure (configuration C) in the rutile phase. The energy differences between configurations C and D for Co, Ni, and Cu doping are, respectively, 0.768 , 0.453 , and 0.179 eV. This indicates that Co has the strongest preference to form a chain structure. Note that if the dopant atoms prefer to remain iso-

lated (configuration D) in the rutile structure, the anatase to rutile phase conversion will not take place. In Co-doped TiO₂, the rutile phase (configuration D) is 0.691 eV higher in energy than the anatase phase (configuration A). Therefore, Co and Ni doping tend to lower the energy of the doped system by maximizing their interaction, and hence forming a linear chain as in the rutile phase.

To see if this indeed is the real mechanism, we carried out systematic calculations on *M*-doped TiO₂ using other 3*d* elements, namely, Cr, Mn, and Fe. Among these Cr has the highest spin moment in the 3*d* series, namely, 6 μ_B , and Mn atom has a spin moment of 5 μ_B . However, due to its half-filled 3*d* and filled 4*s* orbitals (3*d*⁵ 4*s*²) Mn atoms interact weakly with each other and the cohesive energy of bulk Mn is the lowest among the 3*d* transition-metal atoms. Thus, one would expect that Mn doping will result in the least energy gain when Mn atoms form a linear chain in the rutile phase and hence can hardly induce phase conversion in TiO₂. This is exactly what our calculations yielded.

In Fig. 3 we summarize the main results of this Rapid Communication. For 6.25% dopant concentration, no phase conversion is found for any of the dopants. However, for 12.5% concentration Co and Ni induce phase conversion while Cr, Mn, and Cu do not. Fe doping seems to lie at the threshold as the energy difference between the rutile and anatase phases is too small to predict its precise role in phase conversion. Also plotted in Fig. 3 is the energy difference between configurations C and D. In configuration C the dopant atoms in the rutile phase form a linear chain (clustering) while in configuration D, they do not cluster. The variation in this energy is remarkably similar to that of the energy difference between the anatase and rutile phases, giving clear indication that the increased interaction between Co atoms confined to a linear chain in the rutile phase is responsible for the phase conversion.

In summary, we have studied systematically the relative stability between the anatase to rutile phase in transition-metal (*M*)-doped TiO₂ (*M*=Cr, Mn, Fe, Co, Ni, and Cu) and explored the origin of the surprising room-temperature phase conversion in Co and Ni-doped system. The phase conversion is neither induced by the high spin of the dopants nor by the strain. Instead, it depends on the preferred configuration dopant atoms assume in the rutile phase. When the concen-

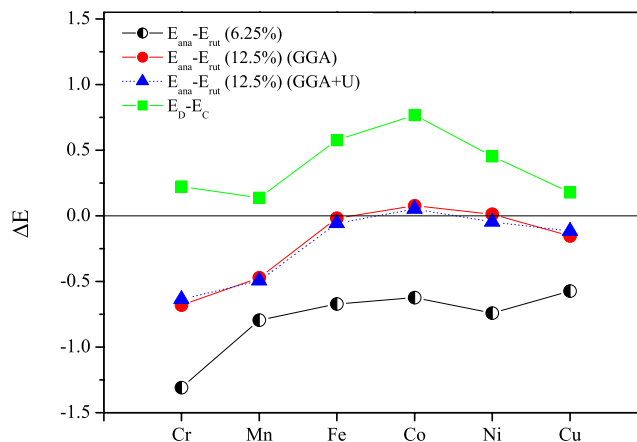


FIG. 3. (Color online) The energy difference ($\Delta E = E_{\text{anatase}} - E_{\text{rutile}}$) between anatase and rutile for *M*-doped TiO₂ (*M*=Cr, Mn, Fe, Co, Ni, and Cu) with 6.25% and 12.5% dopant concentration measured with respect to that of pristine TiO₂. The energy of the rutile structure is set to be zero. The square line is the energy difference ($\delta E = E_D - E_C$) between configurations C and D, which correspond to the energy gain when dopants are confined to linear chain structure in the rutile phase.

tration reached 12.5%, the dopant atoms cluster to form a linear chain in the rutile phase and the increased interaction between Co and Ni atoms in the linear chain configuration compared to other dopants causes the observed phase conversion. Our calculations show that Co is the most suitable dopant due to its largest energy gain in the linear chain structure. We predict that Mn and Cr doping will not be able to cause this phase conversion. It is difficult to predict the role of Fe due to the minor energy difference between the anatase and the rutile phases. Experimental studies of Cr, Mn, and Fe-doped TiO₂ will help establish the accuracy of our prediction.

This research used resources of the National Energy Research Scientific Computing Center, which is supported by the Office of Science of the U.S. Department of Energy under Contract No. DE-AC02-05CH11231. Partial support of this work by the Department of Energy is also acknowledged.

- ¹B. O'Regan and M. Gratzel, *Nature (London)* **353**, 737 (1991).
- ²U. Bach *et al.*, *Adv. Mater.* **14**, 845 (2002).
- ³L. D. Birkefeld *et al.*, *J. Am. Ceram. Soc.* **75**, 2964 (1992).
- ⁴A. Fujishima and K. Honda, *Nature (London)* **238**, 37 (1972).
- ⁵F. Dacheille *et al.*, *Am. Mineral.* **53**, 1929 (1968).
- ⁶T. Ohno *et al.*, *J. Catal.* **203**, 82 (2001).
- ⁷G. H. Li *et al.*, *J. Mol. Catal. A: Chem.* **275**, 30 (2007).
- ⁸D. C. Hurum *et al.*, *J. Phys. Chem. B* **107**, 4545 (2003).
- ⁹Y. H. Zhang and A. Reller, *Mater. Sci. Eng., C* **19**, 323 (2002).
- ¹⁰S. Riyas *et al.*, *Adv. Appl. Ceram.* **106**, 255 (2007).
- ¹¹D. J. Reidy *et al.*, *J. Eur. Ceram. Soc.* **26**, 1527 (2006).

- ¹²J. L. Gole *et al.*, *J. Phys. Chem. C* **112**, 1782 (2008).
- ¹³G. Kresse and J. Furthmuller, *Phys. Rev. B* **54**, 11169 (1996).
- ¹⁴P. E. Blochl, *Phys. Rev. B* **50**, 17953 (1994).
- ¹⁵Y. Wang and J. P. Perdew, *Phys. Rev. B* **44**, 13298 (1991).
- ¹⁶M. S. Park *et al.*, *Phys. Rev. B* **65**, 161201(R) (2002).
- ¹⁷C. E. Rodriguez-Torres *et al.*, *J. Phys.: Condens. Matter* **20**, 135210 (2008).
- ¹⁸T. Umebayashi *et al.*, *J. Phys. Chem. Solids* **63**, 1909 (2002).
- ¹⁹S. Duhalde *et al.*, *Phys. Rev. B* **72**, 161313(R) (2005).
- ²⁰C. E. R. Torres *et al.*, *Appl. Surf. Sci.* **254**, 365 (2007).
- ²¹Q. K. Li *et al.*, *Europhys. Lett.* **81**, 17004 (2008).